

# Cyclotron Resonances in a Non-Neutral Multispecies Ion Plasma

M. Affolter, F. Anderegg, C. F. Driscoll, and D. H. E. Dubin

*Department of Physics, University of California at San Diego, La Jolla, California 92093*

**Abstract.** Shifts of the cyclotron mode frequencies, away from the single particle limit, are observed to be proportional to the measured  $E \times B$  rotation frequency in a non-neutral ion plasma. These cylindrical ion plasmas consist of  $^{24}\text{Mg}^+$ ,  $^{25}\text{Mg}^+$ , and  $^{26}\text{Mg}^+$ ; with  $\text{H}_3\text{O}^+$ , and  $\text{O}_2^+$  impurities. Laser cooling of the  $^{24}\text{Mg}^+$  majority species enables temperature control over the range  $10^{-5} < T < 10^{-2} \text{ eV}$ , as well as determination of cyclotron mode frequencies from launched wave absorption. At moderately low temperatures, the  $m_\theta = 1$  and  $m_\theta = 2$  cyclotron frequency shifts are well described by cold fluid theory for an equilibrium square profile. However, for  $T < 10^{-3} \text{ eV}$ , centrifugal mass separation can shift the mode frequency back towards the single particle limit.

**Keywords:** cyclotron, frequency shift, multispecies, nonneutral plasma

**PACS:** 52.27.Jt, 82.80.Qx, 52.50.Qt, 52.25.Vy

## INTRODUCTION

Plasma effects, such as  $E \times B$  drift rotation, shift the cyclotron mode frequencies away from the single particle limits,  $f_{c,i} = \frac{eB}{2\pi m_i c}$ , for each species  $i$ . This shift has been measured and theoretically explained for single species electron plasmas [1], and has been observed in precision cyclotron mass spectrometry experiments [2, 3]. Previous experiments [4] on multispecies ion plasmas, with parabolic density profiles, obtained shifts that were well explained theoretically only for the majority ion species. In this paper, measurements of the cyclotron mode frequencies, in a rigid rotor multispecies ion plasma, show quantitative correspondence with cold fluid theory for both the majority and minority species.

## EXPERIMENT

The cyclotron modes are observed in a multispecies ion plasma consisting of  $^{24}\text{Mg}^+$ ,  $^{25}\text{Mg}^+$ , and  $^{26}\text{Mg}^+$ ; with  $\text{H}_3\text{O}^+$  and  $\text{O}_2^+$  impurity ions. A cylindrical Penning-Malmberg trap is used to confine the plasma in a field of  $B = 2.96$  Tesla. The plasma is maintained in a near thermal equilibrium state using a rotating wall. This enables variations of the radius,  $0.2 < R_p < 0.4 \text{ cm}$ , density,  $1.8 \times 10^7 < n < 4.7 \times 10^7 \text{ cm}^{-3}$ , and measured  $E \times B$  rotation frequency,  $8.6 < f_{Rot} < 23.0 \text{ kHz}$ ; while the length,  $L_p \sim 10 \text{ cm}$ , and total charge,  $N_q \sim 10^8 e$ , remain constant. Laser cooling of the  $^{24}\text{Mg}^+$  ions enables controlled temperatures over the range  $10^{-5} < T < 10^{-2} \text{ eV}$ . Radial profiles of the plasma temperature, total Mg density, and  $E \times B$  drift velocities,  $v_\theta$ , are obtained using laser induced fluorescence (LIF) techniques [5]. A single number,  $f_{Rot}$ , is obtained by a

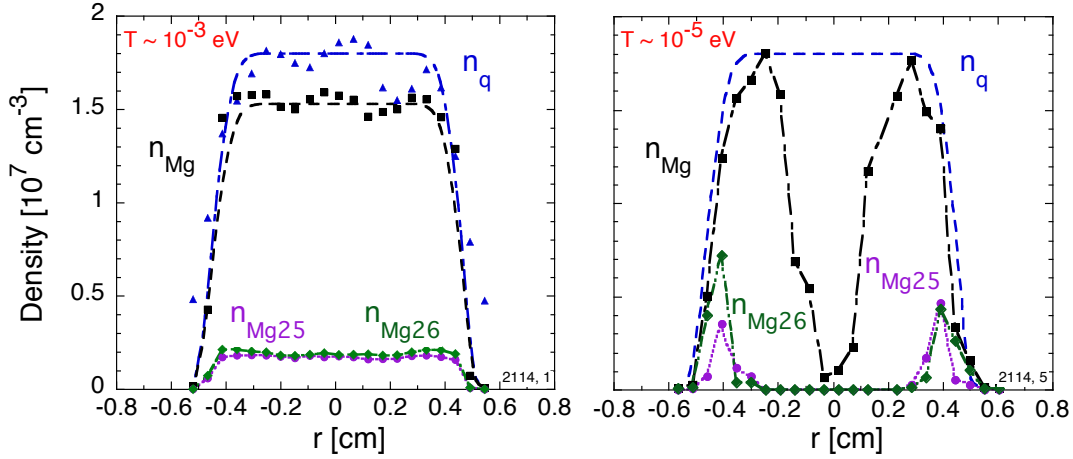


**FIGURE 1.** (Left) Density profile of a warm plasma,  $T \sim 10^{-3} \text{ eV}$ , in which the ion species are well mixed. (Right) Density profile of a cold plasma,  $T \sim 10^{-5} \text{ eV}$ , in which the ion species are centrifugally separated by mass. The Mg density is measured directly using LIF, and the total charge density,  $n_q$ , is calculated from the measured  $E \times B$  rotation profile of the plasma.

linear fit to  $v_\theta(r) = 2\pi r f_{Rot}$ , where  $r$  is the distance from the center of the plasma. When the plasma is cooled to  $T \leq 10^{-3} \text{ eV}$ , the ion species begin to centrifugally separate by mass [6]. A typical warm mixed plasma, and a cold centrifugally separated plasma can be seen in Fig. 1. These plasmas are in a near rigid rotor equilibrium, with a square total charge density profile.

Thermal cyclotron spectroscopy (TCS) is used to measure the cyclotron mode frequencies. A series of rf bursts, scanned over frequency, are applied to an azimuthally sectorized,  $R_w = 2.86 \text{ cm}$ , ring. When the rf burst is resonant with a particular mode at  $f_{res}$ , the plasma is heated, and this is observed as a change in the background laser cooling fluorescence. Figure 2 shows a broad TCS scan, with  $m_\theta = 1$  (dipole) bursts, used to determine the plasma composition. Higher-order cyclotron modes can also be excited by using different azimuthally dependent bursts.

The  $m_\theta = 1$  and  $m_\theta = 2$  modes of  $^{24}\text{Mg}^+$  are shown in Fig. 3. It can be seen from Fig. 3 that the  $m_\theta = 1$  mode is downshifted, while the  $m_\theta = 2$  mode is upshifted from  $f_{c,24} = 1.8986 \text{ MHz}$ . The difference in frequency between these two modes is approximately 10% larger than the measured  $f_{Rot} = 8.9 \text{ kHz}$ . As the plasma is compressed using the rotating wall, increasing  $f_{Rot}$ , the modes shift further from the single particle limit. This shift of the mode frequency is displayed in Fig. 4, for the  $m_\theta = 1$  mode of  $^{24}\text{Mg}^+$ , at three different measured  $E \times B$  rotation frequencies.

Plotted in Fig. 5 are the  $m_\theta = 1$  and  $m_\theta = 2$  cyclotron mode frequencies of  $^{24}\text{Mg}^+$ ,  $^{25}\text{Mg}^+$ , and  $^{26}\text{Mg}^+$  versus  $f_{Rot}$ ; here, all data is from the same trapped ions. A linear shift of the cyclotron mode frequencies with  $f_{Rot}$  is clearly observed. The minority species,  $^{25}\text{Mg}^+$  and  $^{26}\text{Mg}^+$ , are shifted more than the majority species for the  $m_\theta = 1$  mode; and are shifted less for the  $m_\theta = 2$  mode. As  $f_{Rot}$  approaches zero, both the  $m_\theta = 1$  and  $m_\theta = 2$  modes approach  $f_{c,i}$ . These measurements are done at a constant temperature,  $T \sim 2 \times 10^{-3} \text{ eV}$ , where effects of centrifugal separation can be ignored.

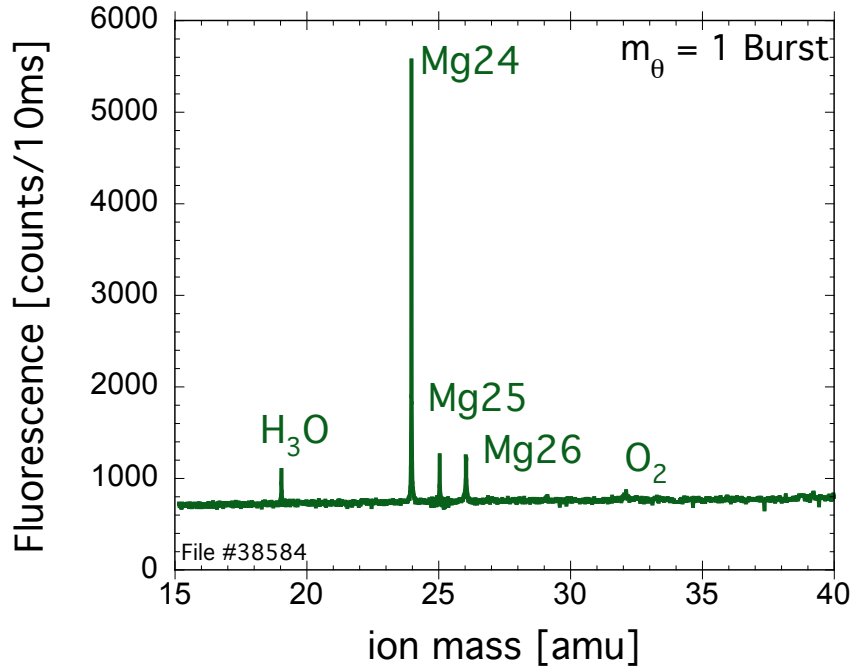


**FIGURE 2.** Mass spectra of a typical plasma containing  $^{24}\text{Mg}^+$ ,  $^{25}\text{Mg}^+$ , and  $^{26}\text{Mg}^+$ ; with  $\text{H}_3\text{O}^+$  and  $\text{O}_2^+$  impurity ions. The burst frequency is scanned from 1.137 MHz to 3.000 MHz to excite ions in this mass range.

A qualitatively different shift of the  $m_\theta = 1$   $^{24}\text{Mg}^+$  mode frequency is observed for  $T \leq 10^{-3}$  eV, due to centrifugal mass separation. As the plasma is cooled, the species begin to centrifugally separate, causing the  $m_\theta = 1$  resonance to increase towards  $f_{c,i}$ . This temperature dependent shift is clearly seen in Fig. 6, where the cyclotron resonance is shown at three different temperatures. Measurements of the mode frequency versus temperature are plotted in Fig. 7. A constant  $E \times B$  rotation frequency of 8.6 kHz was used for these measurements.

## ANALYSIS

The downshifts in the  $m_\theta = 1$  (center of mass) cyclotron modes can be understood through a simple fluid model [7]. Figure 8 shows the cross section of a confined plasma displaced by a small amount  $\Delta$ . Image charge on the conducting cylinder produces an electric field, causing the plasma to  $E \times B$  rotate at the diocotron frequency,  $f_d$ . The force on the plasma from this electric field is anti-parallel to the  $v \times B$  force; this reduces the total radial force on a particle, and hence reduces the  $m_\theta = 1$  cyclotron mode frequency. In a single species plasma the reduction in the radial force is caused only by image charge. For this case, this simple model correctly predicts the downshift of the cyclotron mode by  $f_d$ , as shown by Gould and LaPointe [7]. In a multispecies plasma there is an additional downshift caused by the electric field of the non-resonant charge species.

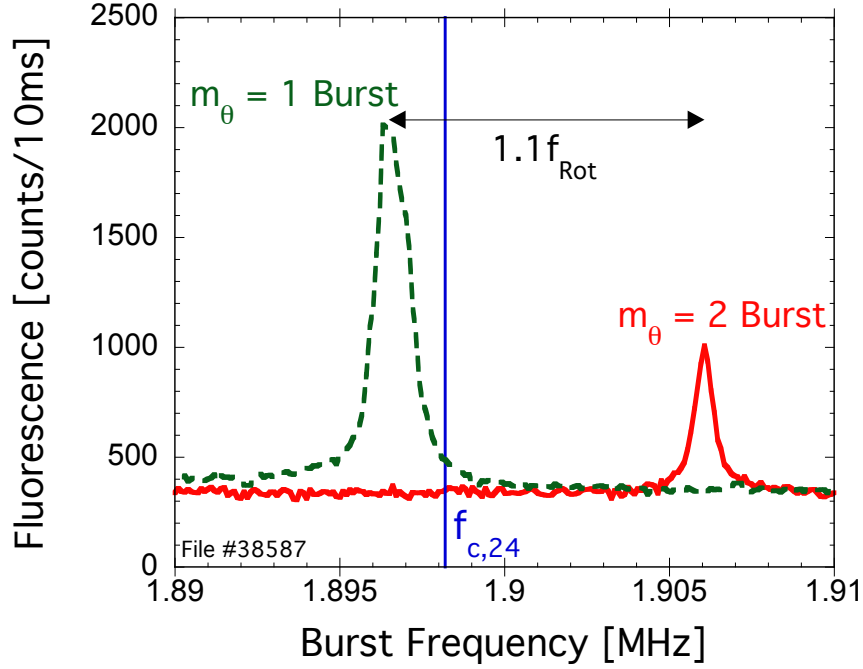


**FIGURE 3.** Detection of the  $m_\theta = 1$  and  $m_\theta = 2$  cyclotron modes of  $^{24}\text{Mg}^+$ . The vertical line marks the  $^{24}\text{Mg}^+$  single particle cyclotron frequency and  $f_{\text{Rot}} = 8.9$  kHz.

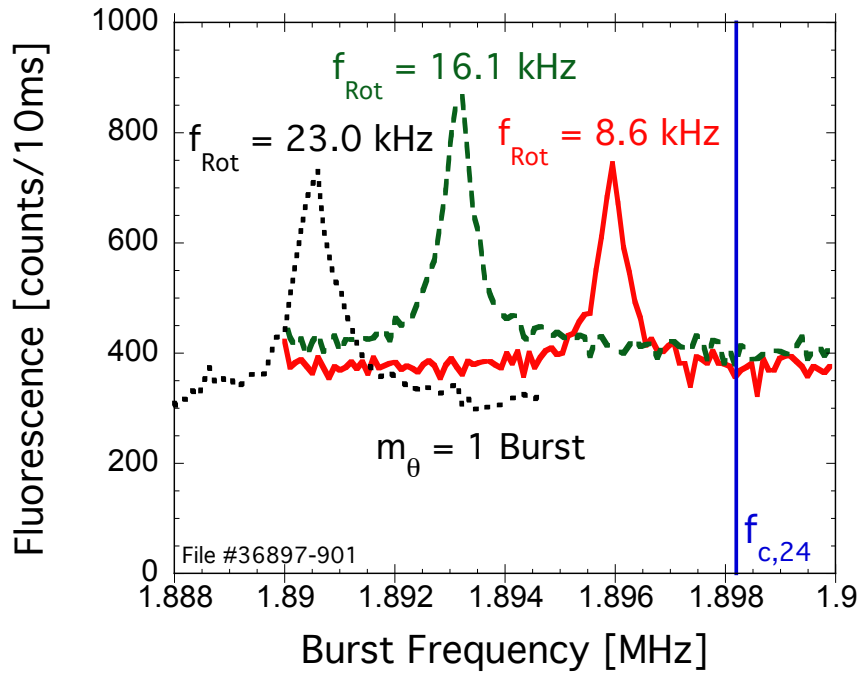


**FIGURE 4.** Shift of the  $m_\theta = 1$  mode for  $^{24}\text{Mg}^+$  at three different measured  $E \times B$  rotation frequencies. As  $f_{\text{Rot}}$  increases, the  $m_\theta = 1$  mode shifts away from  $f_{c,24}$ , the vertical line.

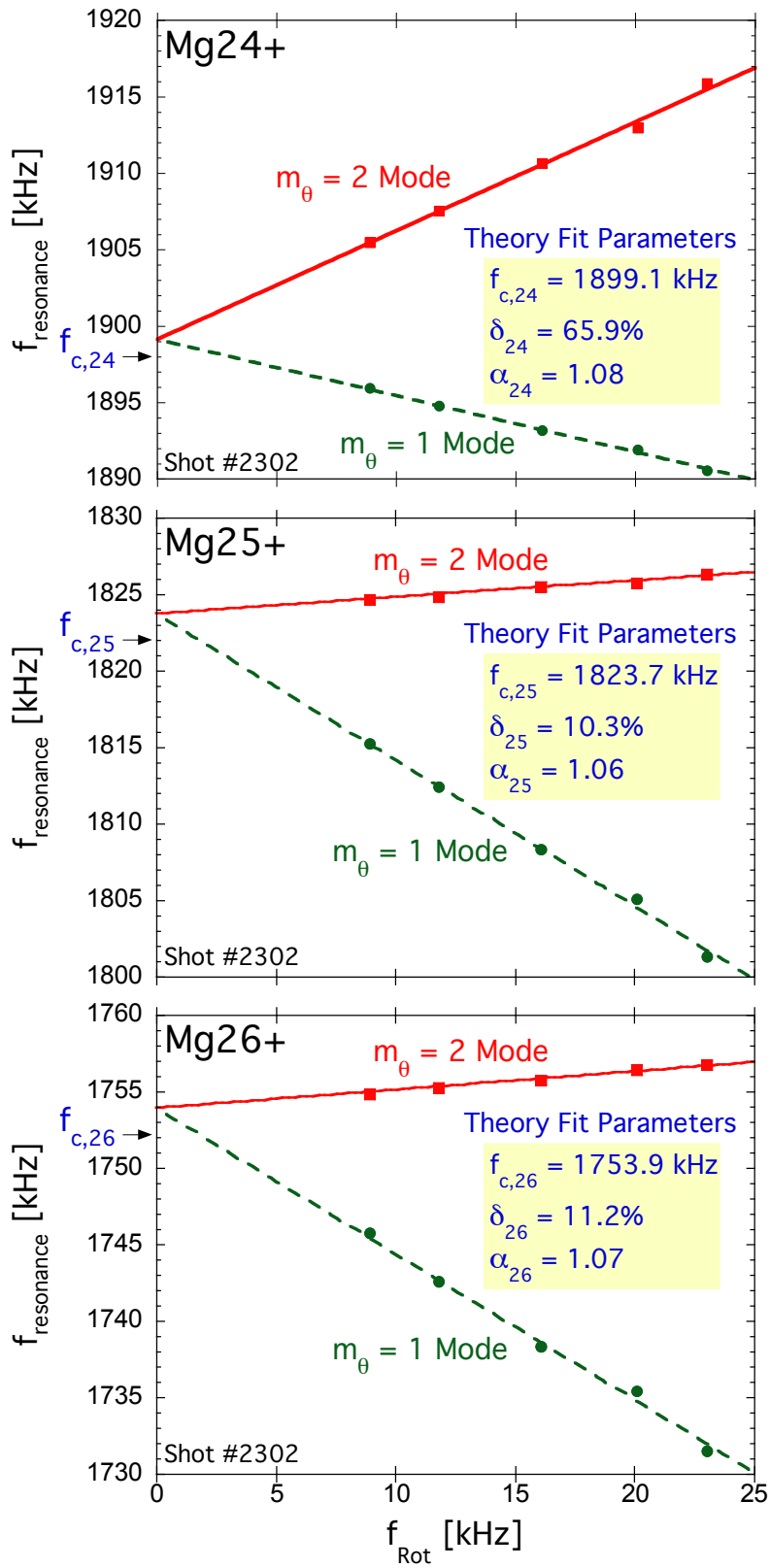


**FIGURE 5.** Frequencies,  $f_{\text{res}}$ , of the  $m_{\theta} = 1$  and  $m_{\theta} = 2$  cyclotron modes plotted versus the measured plasma  $E \times B$  rotation frequency for  $^{24}\text{Mg}^+$ ,  $^{25}\text{Mg}^+$ , and  $^{26}\text{Mg}^+$ . The solid and dashed lines are the theory fit to this data, and the boxes contain the resulting fit parameters.

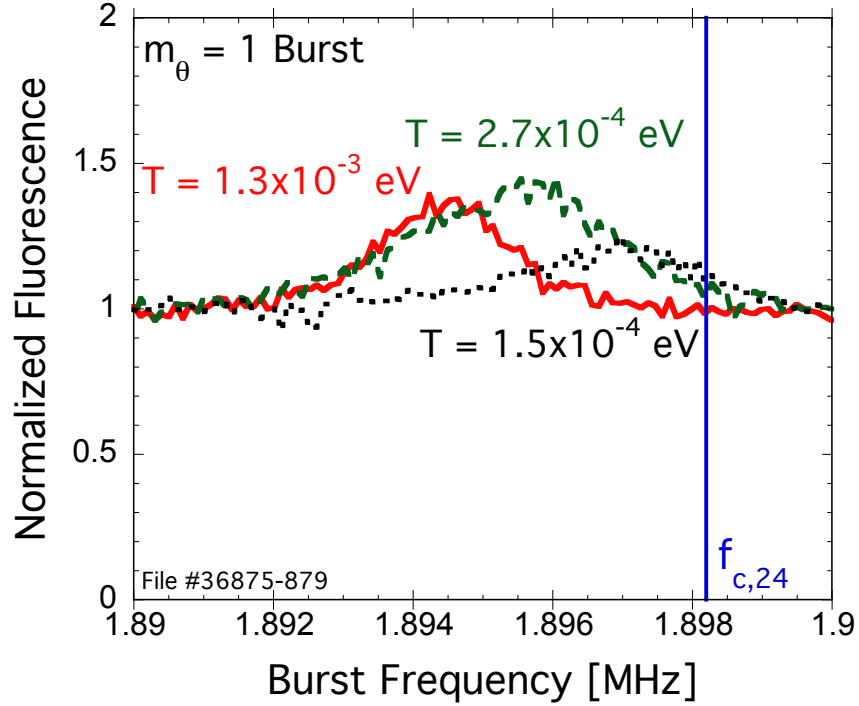


**FIGURE 6.** Shift of the  $m_\theta = 1$  mode for  $^{24}\text{Mg}^+$  at three different temperatures. As the temperature decreases, the  $m_\theta = 1$  mode shifts towards  $f_{c,24}$ , the vertical line.

Cold fluid theory can be used to predict the cyclotron mode frequency in the multispecies case.

Cold fluid theory treats each species as a separate cold fluid moving in the electric field from all species; and each species responds to a burst only at its resonant frequency. In other words, a cyclotron mode consists of a single fluid orbiting at  $f_{res}$  with no drag from the other stationary fluids. Gould [8] established the theory for radial dependent profiles for a two species plasma, and this work was extended by Sarid et al. [4] to an arbitrary number of species. For simplicity, singly charged species have been assumed in the theory. The shift of the mode frequency,  $\Delta f_{m_\theta,i} \equiv \lambda_{m_\theta,i} f_{E \times B}(0)$ , away from the single particle limit is determined by solving for  $\lambda_{m_\theta,i}$ , as

$$-\left(\frac{2m_\theta}{R_w^{2m_\theta}}\right) \int_0^{R_w} dr \frac{\delta_i h(r) r^{2m_\theta-1}}{\lambda_{m_\theta,i} - (m_\theta - 1)g(r) + (1 - \delta_i)h(r)} = 1, \quad (1)$$

where  $f_{E \times B}(0)$  is the 2D cold fluid theory  $E \times B$  rotation frequency at  $r = 0$ ,  $h(r)$  and  $g(r)$  are the density and rotation profiles (normalized to  $r = 0$ ), and  $\delta_i = q_i n_i / \sum q_i n_i$  is the relative charge fraction of species  $i$ . For the  $m_\theta = 1$  mode in a single species plasma, Eq. (1) reduces to

$$-\frac{1}{\lambda} \left(\frac{2}{R_w^2}\right) \int_0^{R_w} dr h(r) r = -\frac{\langle h(r) \rangle}{\lambda} = 1, \quad (2)$$

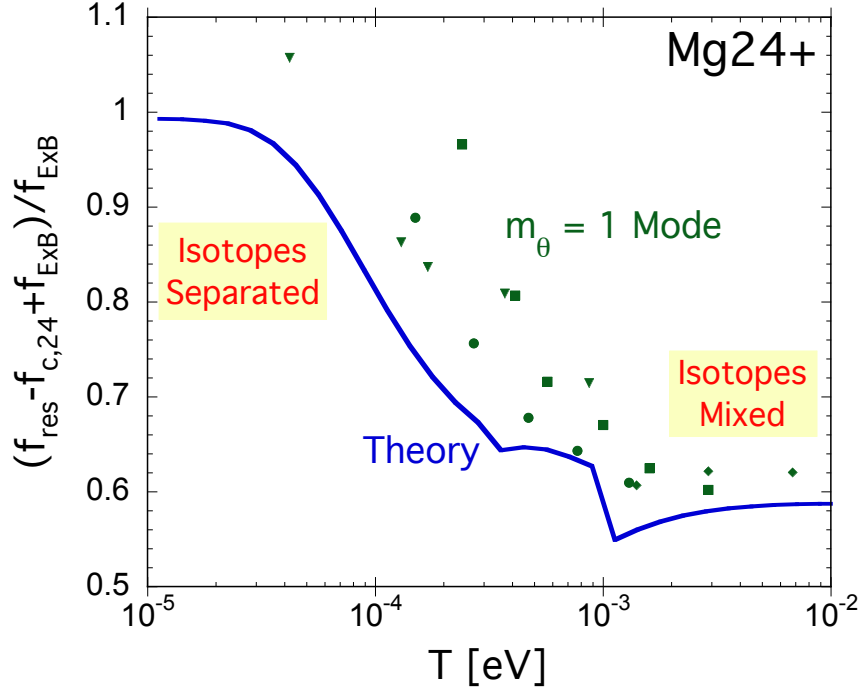


**FIGURE 7.** Measured frequency shift of the  $m_\theta = 1$  mode for  $^{24}\text{Mg}^+$  versus the plasma temperature. Also plotted is the solution from a theory model in which these shifts are caused by centrifugal separation of the ion species, the solid line.

so the shift of the cyclotron mode is

$$\Delta f_1 = -f_{E \times B}(0) \langle h(r) \rangle = -f_d, \quad (3)$$

as seen from the simple model. Here, the cyclotron resonance is independent of the plasma profile; but this is not the case for  $m_\theta > 1$  or for a multispecies plasma.

Note that for the  $m_\theta = 1$  mode in a multispecies plasma, the denominator in Eq. (1) may vanish where  $h(r) = |\lambda_i|/(1 - \delta_i)$ . In this case, Eq. (1) is not analytically tractable, since it does not properly model wave absorption at a resonant radius. This occurs for the minority species in a plasma with a parabolic density profile, explaining the lack of a theory comparison for these species in the previous work of Sarid et al. [4] The downshift of  $f_{c,i}$  by  $2f_d$  observed by Sarid et al. [4] for the minority species is most likely a shift of  $f_{E \times B}$  scaled by effects of the profile shape.

The resonant radius absorption problem becomes less relevant for cold plasmas where  $h(r)$  approaches a square profile. For a square profile, with unique rotation frequency  $f_{E \times B}$ , Eq. (1) can be solved to obtain the shift in the cyclotron mode frequency for both the majority and minority species as

$$\Delta f_{m_\theta, i} = f_{E \times B} \left\{ (m_\theta - 2) + \delta_i \left[ 1 - \left( \frac{R_p}{R_w} \right)^{2m_\theta} \right] \right\}. \quad (4)$$

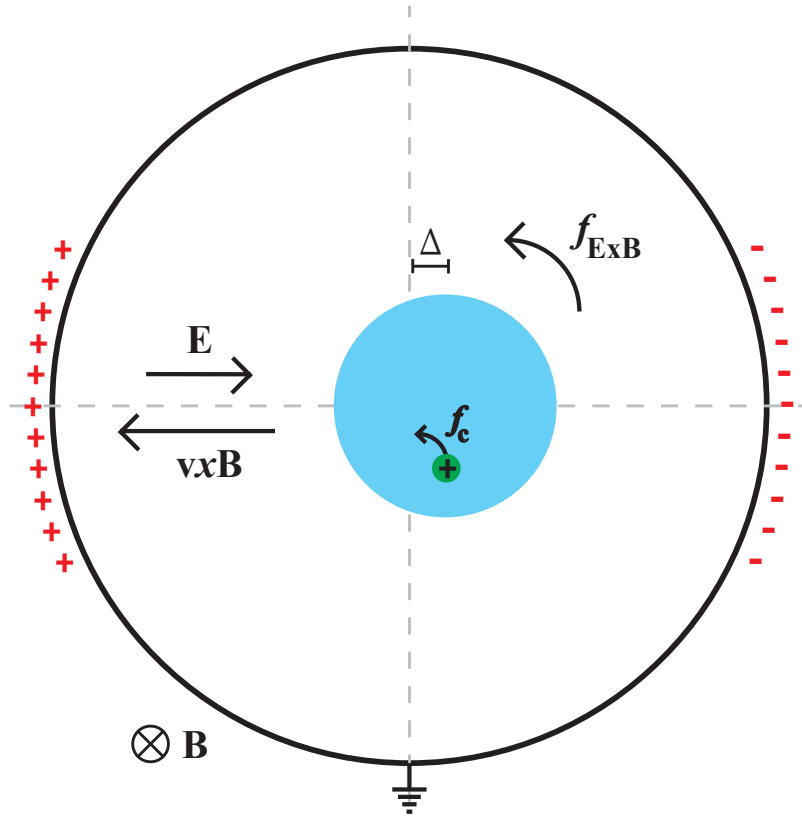


**FIGURE 8.** Sketch illustrating the effect of an electric field on the  $m_\theta = 1$  cyclotron mode frequency.

For a single species plasma ( $\delta_i = 1$ ) the downshift of  $f_d$  caused by image charge is recovered. Image charge effects are negligible for the multispecies plasma presented here, since  $\left(\frac{R_p}{R_w}\right)^{2m_\theta} \ll 1$ . Ignoring the image charge term, the frequency shifts reduce to

$$\Delta f_{1,i} = (\delta_i - 1)f_{E \times B} \quad (5)$$

for the  $m_\theta = 1$  mode; and

$$\Delta f_{2,i} = \delta_i f_{E \times B} \quad (6)$$

for the  $m_\theta = 2$  mode.

Cold fluid theory predicts, in agreement with the experimental results, that the  $m_\theta = 1$  and  $m_\theta = 2$  cyclotron modes are linearly dependent on  $f_{E \times B}$ . The downshift of the  $m_\theta = 1$  mode, and upshift of the  $m_\theta = 2$  mode from  $f_{c,i}$  is also correctly predicted. Since the size of the frequency shift is dependent on  $\delta_i$ , the relative charge fraction of species  $i$ , the majority and minority species are shifted by different fractions of  $f_{E \times B}$ , which is clearly seen in the data.

Equation (5) and (6) are the fit lines shown in Fig. 5, with  $f_{E \times B} = \alpha_i f_{Rot}$ . The parameter  $\alpha_i$  represents a possible difference between the experimentally fitted  $E \times B$  rotation frequency,  $f_{Rot}$ , and the theory model,  $f_{E \times B}$ . Typically, the fit giving  $f_{Rot}$  is considered accurate to  $\pm 5\%$  for these cold plasmas with measured  $v_\theta(r) \propto r$ . The



three parameter linear fits in Fig. 5 determine  $f_{c,i}$ ,  $\delta_i$ , and  $\alpha_i$  for each species. The single particle cyclotron frequencies obtained from these fits are within 0.1% of  $f_{c,i}$  calculated from the magnetic field. These fits also allow for a measurement of the charge fractions  $\delta_{Mg25}/\delta_{Mg24} = 15.9\%$  and  $\delta_{Mg26}/\delta_{Mg24} = 17.0\%$ , which are within 5% of those obtained from LIF techniques. The constancy of  $\alpha_i \sim 1.07$  for the three species suggests an issue with either 2D cold fluid theory, which ignores z-dependence and end effects, or with the experimental fits to obtain  $f_{Rot}$ .

The discussion so far has all been for a plasma at a temperature where the effects of centrifugal separation can be ignored. As the plasma temperature is lowered, the species begin to centrifugally separate, resulting in different density profiles for each species. This causes a shift of the cyclotron resonance, since the mode frequency is dependent on the charge distribution of each species. By numerically solving the cold fluid equations for a centrifugally separated plasma; Dubin was able to calculate a temperature dependent shift. Plotted in Fig. 7 is the measured shift versus temperature, and the numerical results for the  $m_\theta = 1$  cyclotron mode frequency of  $^{24}\text{Mg}^+$ .

## CONCLUSION

The cyclotron mode frequency in a non-neutral plasma is shifted away from the single particle limit due to plasma effects. In a single species plasma this shift is caused by the electric field created from image charge, and results in a shift of  $f_d$ . For a multispecies plasma both the electric field from image charge, and the electric field from other charge species shift the cyclotron modes. Cold fluid theory correctly predicts these shifts in a multispecies plasma with a square density profile. When the effects of image charge can be ignored, these shifts can be used to determine the relative charge fraction of each species. The shape of the plasma profile also shifts the cyclotron resonances, so centrifugal separation causes a temperature dependent shift.

## ACKNOWLEDGMENTS

This work was supported by National Science Foundation Grant No. PHY0903877 and Department of Energy Grant DE-SC0002451.

## REFERENCES

1. R. W. Gould and M. A. LaPointe, Phys. Rev. Lett. **67**, 3685-3688 (1991).
2. C. Masselon, A.V. Tolmachev, G.A. Anderson, R. Harkewicz and R.D. Smith, J. Am. Soc. Mass Spectrom **13**, 99-106 (2002).
3. M.L. Easterling, T.H. Mize and I.J. Amster, Anal. Chem. **71**, 624-632 (1999)
4. E. Sarid, F. Anderegg and C. F. Driscoll, Phys. Plasmas **2**, 2895-2907 (1995).
5. F. Anderegg, X.-P. Huang, E. Sarid and C. F. Driscoll, Rev. Sci. Instrum. **68**, 2367-2377 (1997).
6. G. B. Andresen, M. D. Ashkezari, M. Baquero-Ruiz, W. Bertsche, Paul David Bowe, E. Butler, C. L. Cesar et al. Phys. Rev. Lett. **106**, 145001 (2011).
7. R. W. Gould and M. A. LaPointe, Phys. Fluids B **4**, 2038-2043 (1992).
8. R. W. Gould, Phys. Plasmas **2**, 1404-1411 (1995).